Ion Homeostasis in Rhythmogenesis: The Interplay Between Neurons and Astroglia

Aklesso Kadala, Dorly Verdier, Philippe Morquette, Arlette Kolta

PHYSIOLOGY 30: 371–388, 2015; doi:10.1152/physiol.00023.2014

Ion Homeostasis in Rhythmogenesis: The Interplay Between Neurons and Astroglia

Aklesso Kadala,[1] Dorly Verdier,[1] Philippe Morquette,[1] and Arlette Kolta[1,2]

[1]*Département de Neurosciences and Groupe de Recherche sur le Système Nerveux Central, Université de Montréal, Montréal, Québec, Canada; and* [2]*Faculté de Médecine Dentaire and Réseau de Recherche en Santé Bucco-dentaire et Osseuse du Fonds de Recherche Québec-Santé, Université de Montréal, Montréal, Québec, Canada*
Arlette.kolta@umontreal.ca

Proper function of all excitable cells depends on ion homeostasis. Nowhere is this more critical than in the brain where the extracellular concentration of some ions determines neurons' firing pattern and ability to encode information. Several neuronal functions depend on the ability of neurons to change their firing pattern to a rhythmic bursting pattern, whereas, in some circuits, rhythmic firing is, on the contrary, associated to pathologies like epilepsy or Parkinson's disease. In this review, we focus on the four main ions known to fluctuate during rhythmic firing: calcium, potassium, sodium, and chloride. We discuss the synergistic interactions between these elements to promote an oscillatory activity. We also review evidence supporting an important role for astrocytes in the homeostasis of each of these ions and describe mechanisms by which astrocytes may regulate neuronal firing by altering their extracellular concentrations. A particular emphasis is put on the mechanisms underlying rhythmogenesis in the circuit forming the central pattern generator (CPG) for mastication and other CPG systems. Finally, we discuss how an impairment in the ability of glial cells to maintain such homeostasis may result in pathologies like epilepsy and Parkinson's disease.

Proper neuronal function depends critically on the ability of neurons to encode information by changing their firing pattern. Whether a neuron unfailingly transmits spike trains or generates an oscillatory burst firing in response to a given incoming input will bestow different encodings to the conveyed information and result in totally distinct output signals that have different functional incidence. In several brain areas, neurons have been shown to display a function-related dual mode of firing, alternating between a single spike firing mode and a rhythmic burst pattern (67, 92, 98, 111, 139). The role and necessity of such rhythmic neuronal discharges is obvious for some functions such as repetitive movements like mastication, locomotion, or breathing. Indeed, for rhythmic movements to occur, repetitive motor output commands are required to produce the appropriate rhythmic contractions of the skeletal muscles involved in their execution. This implies a need for coordinated discharges by the central pattern generators (CPGs) to initiate and maintain the rhythmic output of motoneurons. Nevertheless, rhythmic activities are also observed in several areas of the brain where their function is not clearly related to a rhythmic behavior but rather to functions such as the binding of sensory features in perception (51, 93), cognitive processing (91), information transfer between brain areas (131), learning and memory (138), sleep and consciousness (38), or motor coordination (79, 84). In fact, neuronal oscillatory activity appears to be an ubiquitous phenomenon in the brain, with wide-ranging functions that occur along with normal brain processing (for review, see Ref. 159).

The mechanisms underlying the transition from single spike firing to rhythmic bursting are not fully understood yet. However, considering the critical importance of ion homeostasis for an optimal neural function, an obvious way to impact on the neuronal firing properties would be to modulate the ionic concentration in the extracellular compartment. Indeed, in several studies where the ions concentrations were measured directly in the tissue, variations in extracellular ion concentrations occurred before or simultaneously with rhythmic neuronal discharges (3, 4, 19). Moreover, artificially decreasing the concentration of extracellular calcium triggers rhythmic firing in masticatory and locomotor central pattern generator neurons (20, 149).

Astrocytes have been shown to modulate neuronal activity by a variety of mechanisms, but one of their most well established functions is to maintain ion homeostasis. Moreover, astrocytes are well positioned in terms of their structural organization relative to neurons to monitor the extracellular space content. Thus here we review the evidence suggesting that astrocytes may play a determinant role in setting the firing mode of adjacent neurons through regulation of the extracellular ionic concentrations.

In the upcoming sections, we will discuss how the concentration of different ion species evolves during rhythmic oscillations. This review will put a special emphasis on potassium and calcium, which are the most considered ions in studies interested in the generation and maintenance of rhythmic oscillations. Evidence supporting a role for glial cells in the generation of rhythmic firing in both healthy and pathological conditions will also be discussed.

Rhythmic Oscillations

Rhythmogenesis

Rhythmogenesis is the cellular process by which a rhythmic mode of firing or burst is generated at the cellular level. For the sake of clarity, we define bursts as recurrent clusters of action potentials occurring at short interspike intervals overriding a plateau-like depolarization and separated by relatively short periods of repolarization (see FIGURE 1A). Consequently, the main characteristic of the bursting pattern is its marked periodicity by contrast to the tonic spiking mode, which consists in the firing of single action potentials that may be occasional or repetitive but lack the apparent recurrent on/off phasic features and often occur at lower frequencies than the firing overriding the plateaus that compose the bursts. Rhythmic clustering of neuronal discharge is sometimes also named neural oscillations and, under this terminology, refers as well to the oscillatory activity of individual neurons or to the large-scale brain oscillations that result from recurrent activity in groups of neurons. These large-scale brain oscillations can be detected locally with field potential recordings or measured outside the scalp by electroencephalograms (EEGs) and are more evocative of the state or degree of firing synchronicity in and between groups of neurons throughout the brain. This supposes that these oscillations, in some situations, may arise from a window of specific spatio-temporal configurations of the spiking activity of individual neurons within a group without an absolute requirement for rhythmic bursting in activity of single cells. Nevertheless, numerous studies have established irrefutable links between the large-scale brain oscillations and membrane potential fluctuations or rhythmic clustering of action potentials firing in individual neurons (78, 144). This suggests that, in many cases, these large-scale brain oscillations may depend on the generation of a rhythmic firing pattern at the cellular level. In fact, it has been postulated that bursting neurons might serve as pacemaker in network oscillations (29). Consequently, in this review, we will discuss and use the term rhythmogenesis to refer both to the generation of rhythmic patterns of action potentials at the cellular level and to the generation of the large-scale brain oscillations.

Ionic Basis of Rhythmogenesis

The precise mechanisms leading to rhythmogenesis vary from one network to another and depend on an intricate interplay between synaptic and intrinsic properties in neuron populations. Many theories have been proposed to explain the generation of oscillatory activity, including synaptic interactions and feedback connections within and between neuronal populations and their contribution to different known frequency bands (159). However, in this review, we will focus on intrinsic neuronal properties that rely on ionic conductances to generate rhythmic firing.

Some of these conductances constitute the driving forces that initiate the burst firing, whereas others determine the plateau duration and bursting frequency or are part of the regenerative feature that characterizes this mode of firing (57). The persistent sodium current (I_{NaP}) is one of the most common currents that drives bursting. Unlike the transient sodium current, which appears at membrane potentials close to −50 mV (21), I_{NaP} becomes apparent at membrane potentials between −65 and −50 mV, and peaks at membrane potentials between −40 and −35 mV, depending on the structure considered (21, 28, 100, 152). Some of the persistent current originates from the same pool of channels as the transient sodium current but with different gating modes (2), and in some other cases, as in the cerebellar Purkinje cells (156), it results from distinctive pools of channels. The massive entry of sodium ions into the cells causing the persistent sodium current supports depolarizing plateaus that are crucial for rhythmic bursting in some neurons. Evidence supporting a role for I_{NaP} in the generation of bursts came from computational simulations (68, 132) and experimental recordings from the pre-Bötzinger complex (PBC) (36, 37), the main sensory nucleus of the trigeminal nerve (20, 152), the spinal cord (149), the cortex (23, 54, 110), or the hippocampus (72, 146). In these experiments, blockade of I_{NaP} prevented burst firing. I_{NaP} also contributes to large-scale oscillations like those

in the rat's visual cortex, where its blockade significantly reduces the frequency of fast gamma oscillations (113).

Other drivers of burst firing include the low-threshold voltage-activated calcium channels (LVA) and the calcium-activated non-selective cationic channels (driving I_{CAN}). The LVA calcium channels are found in a wide range of cell types, including neurons and muscle fibers, and are generally activated by small voltage changes (6, 12) near the resting potentials of the membrane they are embedded in. The LVA calcium channels (mainly formed by the CaV3 family) mediate the T-current (I_T) responsible for the low-threshold calcium spikes responsible for burst firing and low-frequency oscillations in the thalamus and the cerebellum (for review, see Refs. 66, 120). At rest, the LVA calcium channels are in an inactivated state and require membrane hyperpolarization to be de-inactivated, allowing their subsequent activation upon membrane depolarization. Activation of the LVA calcium channels by a subsequent depolarization causes a massive entry of calcium ions into the cell that generates sufficient depolarization to reach threshold and drive a train of Na^+-dependent action potentials. Whole-cell and extracellular recordings in the thalamus of mice knocked out for CaV3.2 and CaV3.3 clearly show the role that these channels play in regard to rhythmic bursting activity. In these experiments, periodic bursts were absent or significantly reduced in thalamic neurons for CaV3.3 KO mice (7), and simultaneously reduced and increased in the reticular and ventroposterior thalamic neurons, respectively, for mice devoid of CaV3.2 (88). The tonic discharges were unchanged (7). CaV1.3 calcium channels, members of the CaV1 family, could also contribute to burst firing. These channels, which are part of the L-type calcium channels, have been classified as high-voltage-activated (HVA) calcium channels, although they display, in reality, a very low voltage of activation (around −55 mV) (162). They are mostly known to contribute to pacemaking in cardiac atrial tissue and adrenal chromaffin cells but may also play a role in neuronal bursting activity (89, 122).

The channels driving I_{CAN} are activated by the mobilization of intracellular calcium. These channels are seemingly part of the transient receptor potential (TRPM) family, which includes TRPM4 and TRPM5. They are mainly permeable to potassium and sodium but very little to calcium (83, 154). I_{CAN} is responsible for prolonged plateaus (10, 164) seen during rhythmic bursting in several types of cells, although they have no inherent voltage dependency. The contribution of these channels to bursting was confirmed with mathematical models (130), and in many experimental preparations including the reticular thalamic neurons in the guinea-pig (10), the hypothalamic magnocellular neurosecretory cells in the rat (50), the motoneurons of the crab cardiac ganglion (123), the motoneurons of the crab stomatogastric ganglion (164), the main sensory nucleus of the trigeminal nerve (152), and a subset of respiratory neurons in the PBC (116, 119) in which rhythmic firing is abolished by a blocker of I_{CAN} (flufenamic acid) but not by a blocker of I_{NaP} (riluzole) (37, 119). Similar results were reported from investigations in dopaminergic neurons of mice substantia nigra pars compacta (102).

Different types of potassium currents also contribute to bursting activities, mostly by affecting the plateau duration and the bursting frequency. A Na^+-activated potassium current [$I_{K(Na)}$] contributes to the generation of the afterhyperpolarization potential and the maintenance of rhythmic bursts in rat neocortical neurons (48). It was also suggested that Ca^{2+}-dependent potassium currents [$I_{K(Ca)}$] and a muscarine-inhibited M current (I_M) mediated by activation of the Kv7 channels may modulate the firing frequency and contribute to the burst termination in lamprey's spinal cord neurons and rat CA1 pyramidal cells (44, 53). Blocking or opening the small-conductance potassium channels (SK) with apamin or 1-ethyl-2-benzimidazolinone (1-EBIO), respectively, resulted in modulation of the bursting activity in the dopaminergic neurons of the substantia nigra of rats (71).

Finally, other currents, carried by mixed ionic charges, are sometimes at play and contribute mostly to the regenerative feature of this firing mode. As an example, the electrogenic sodium/potassium pump (Na^+-K^+-ATPase) may hyperpolarize neurons and lead to activation of I_h, a cationic current activated by hyperpolarization, which may provide the depolarizing rebound required to reactivate the driving forces for the next burst of action potentials (32). I_h is often revealed by the occurrence of a depolarizing sag in response to increasing hyperpolarization. This current, carried by sodium and potassium ions, has been associated to pacemaker properties in a number of neurons (for examples and review, see Refs. 27, 90, 126).

Sequence of Events Leading to Bursts

How these various conductances interact to promote rhythmogenesis may differ from one area of the brain to another, or even within one brain structure from neuron to neuron. Even at the single-cell level, subcellular localization of different ionic channels in different cell compartments may lead to plural bursts driving modes, as it has been proposed in Purkinje cells that showed two kinds of burst firings with distinctive waveforms; a

somatically generated burst firing driven by activation of sodium persistent channels present on the soma and a dendritically generated burst firing driven by activation of LVC channels that could be found on the dendrites (47).

However, the generation of bursts presents a common sequential scheme that requires *1*) a depolarizing current to produce the plateau potential, *2*) the intervention of a repolarizing process to terminate the burst, and *3*) the need for a depolarizing rebound to reactivate the driving force for the next burst (see FIGURE 1A).

Many models have been proposed to summarize the interplay of conductances leading to the generation of a bursting activity in neurons, and this interplay is merely dependent on the set of channels that are comprised in the cell membrane. In masticatory, respiratory, and locomotor CPGs, the

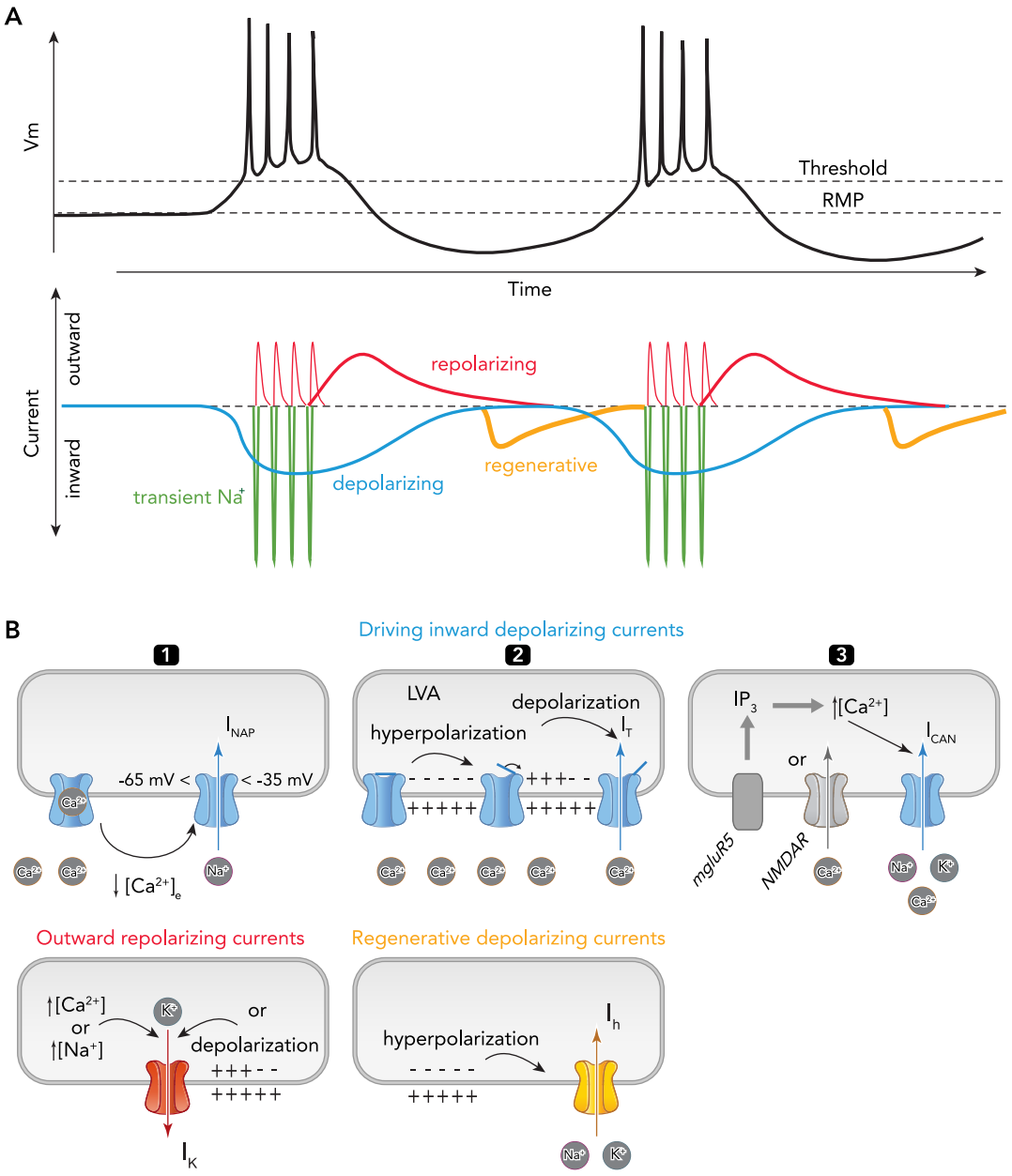

FIGURE 1. **Ionic currents underlying repetitive bursting**
A: representation of two bursts (*top*) and the sequence of activation of the underlying ionic currents (*bottom*). Repetitive bursting generally relies on activation of a conductance that produces a sustained depolarization or plateau (blue) and "drives" the membrane potential from the resting level (RMP) to the threshold for activation of transient sodium currents (dark green) responsible for action potentials. Voltage-gated potassium channels (red) repolarize the membrane after each of these action potentials, whereas other potassium channels activated by Ca^{2+} and Na^{+} entering the cell during depolarization and firing slowly repolarize the membrane often to a level below RMP. In many instances, the hyperpolarization triggers activation of I_h, which enables regeneration (yellow) of the cycle by depolarizing the membrane potential and allowing for reactivation of the driving current. *B*: *top*: different channels responsible for driving the depolarizing plateaus supporting bursting and the conditions required for their activation. *Bottom*: channels required for repolarization and burst termination (red; *left*) and for regenerating the depolarizing drive (yellow: *right*).

observation that the depolarization before bursting activity occurs at membrane potential close to the potential of activation of I_{NaP} and the fact that bursts are abolished upon application of riluzole prompted I_{NaP} as the primary driver of the neuronal bursts (see FIGURE 1B1) (20, 36, 149, 152). Since I_{NaP} is voltage-dependent, the depolarization brought up by its activation would eventually cause its inactivation. In these cells, repolarization and burst termination can be triggered by activation of $I_{K(Na)}$ and/or $I_{K(Ca)}$, which contribute to the burst termination in the rat main sensory trigeminal nucleus (20) as they do in the lamprey spinal cord (44). Voltage-gated potassium channels are also present in the lamprey spinal cord, and their blockade induces an increase in burst frequency (61), making them good candidates for the modulation of the burst cessation. Activation of all these potassium channels would lead to membrane hyperpolarization, which in turn would activate I_h in cells carrying this channel, thus providing for a regenerative drive. In ferret's thalamo-cortical neurons (90) and rat's hippocampal CA3 region (27), blockade of I_h with ZD 7288 abolished both the afterdepolarization and the progressive rebound depolarization and resulted in suppression of the oscillatory activity in these neurons.

In thalamo-cortical neurons, the sequence of events leading to bursting (FIGURE 1B2) is thought to begin with a hyperpolarization that releases LVA calcium channels from their inactivated state, making them available for activation upon depolarization, which may result from activation of I_h by the prior hyperpolarization and which would also trigger firing through the recruitment of sodium and high-voltage-activated calcium channels. The latter eventually activates calcium-dependent potassium channels and voltage-gated potassium channels, which repolarize the plasma membrane and hyperpolarize it to a level sufficient to activate I_h and drive a new boost of depolarization, leading to a renewed activation of calcium conductances (46). In this example, low-voltage-activated calcium channels are clearly the primary driver of the events leading to bursting.

As to bursts driven by I_{CAN} (FIGURE 1B3), Pace and colleagues (116) proposed two different mechanisms. The first one involves metabotropic mGluR5 receptors, which would initiate a process leading to the release of calcium from the intracellular stores through IP_3 receptors. The released calcium would then activate I_{CAN} channels. The second hypothesis involves calcium entry through NMDA receptors. Both mechanisms imply that a synaptic input would activate these channels. No indication was given as to the burst termination; however, like in the lamprey spinal cord, potassium conductances may play that role (44, 61).

Astrocytes are Involved in Ions Homeostasis and Rhythmogenesis

The most studied ions with regard to neuronal excitability and which concentrations are under strict regulation in the brain are potassium, calcium, sodium, and chloride. Potassium concentration is higher in the neuronal intracellular compartment than in the extracellular space (130 mM vs. 2.7-3.5 mM, respectively) (76), whereas the opposite is true for sodium (extracellular and intracellular concentrations are ~145 and 8–15 mM, respectively) (129). Calcium shows the highest difference with an intracellular "resting" concentration of ~100 nM and an extracellular concentration of 1–2 mM (35, 59, 109, 145). The extracellular chloride concentration ($[Cl^-]_e$) is ~120 mM (77), whereas chloride intracellular concentration is between 5 and 20 mM, and is maintained by several molecular elements, including the cation-chloride cotransporters (NKCCs for example) and Cl-HCO_3 exchangers (49, 118).

At rest or relatively low activity levels, neuronal ion pumps and transporters counteract any major ion movements and contribute to maintain the cell membrane at a relatively stable potential as well as the ionic gradient concentrations between the intra- and extracellular compartments. However, with higher activity levels, ionic concentration changes occur in both the intra- and extracellular compartments, and additional mechanisms may be required to restore homeostasis. Evidence suggests that astrocytes may play a major role in controlling the extracellular concentration of some ions.

Potassium

Astrocytes and potassium homeostasis. During neuronal discharge, activation of the voltage-gated potassium channels causes potassium ions to flow toward the extracellular space. The extracellular potassium concentration ($[K^+]_e$) can increase up to a ceiling level of ~12 mM (40) in physiological conditions. Astrocytes are responsible for bringing $[K^+]_e$ back to resting values after an activity-driven increase. In 1966, Orkand et al. (115) introduced the concept of spatial buffering as a possible way of balancing $[K^+]_e$. They proposed that the potassium accumulated during neuronal activity is taken up by neighboring astrocytes and redistributed through the syncytium to less concentrated areas. This is done mainly through the activation of gap junctions (136, 161). Indeed, it has been shown that gap-junctional coupling between astrocytes is increased by elevations in $[K^+]_e$ (34, 45), providing an anatomical support to this theory. Glial cells express several voltage-dependent potassium channels [inward rectifier (Kir); delayed rectifier

(K_d); transient A-type (K_A); Ca^{2+}-activated (K_{Ca})] (for review, see Refs. 11, 25). However, the potassium channel that is predominantly responsible for the high potassium permeability and the maintenance of glial resting membrane potential (RMP) close to the equilibrium potential of potassium (E_K) is Kir, mostly the Kir4.1 channel. Because of the high permeability of glial membrane to potassium, this regulation of $[K^+]_e$ is done mainly by a passive mechanism. However, in some cases, especially when there is an entry of sodium in the glia, an active process that relies on the action of glial Na^+-K^+-ATPase may be at play. In fact, according to D'Ambrosio et al. (31), both Kir channels and the Na^+-K^+ pump participate in the regulation of $[K^+]_e$. Their findings suggest that neuronal and glial Na^+-K^+ pumps may be involved in the setting of baseline $[K^+]_e$ levels and its recovery

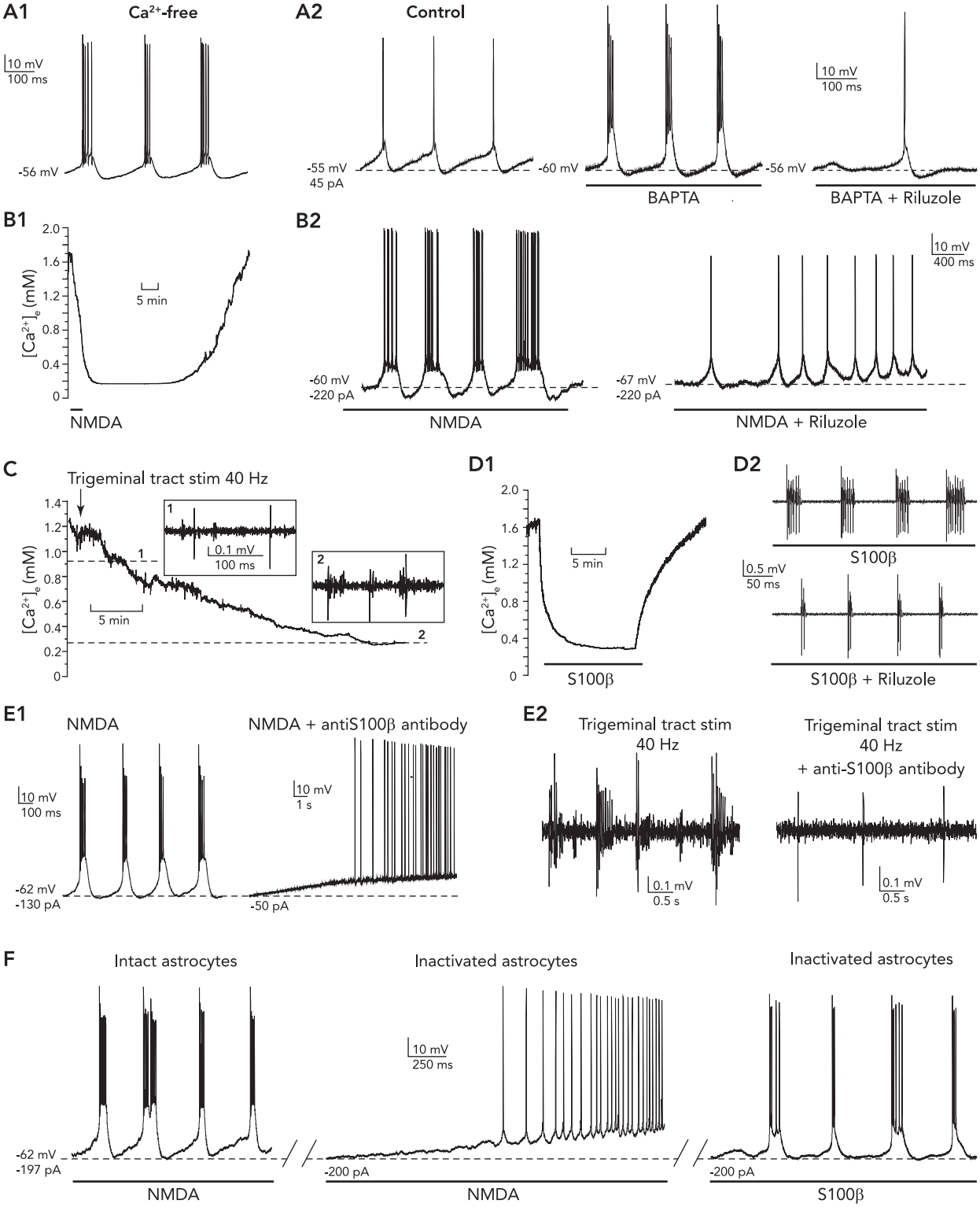

rate during sustained high-frequency firing. Glial Kir channels would also be involved in the regulation of baseline $[K^+]_e$ but might not affect the rate of potassium clearance during neuronal firing. Closely linked to the Kir4.1 channels are the aquaporins-4 (AQP4): membranous channels that allow water flux through the membrane of astrocytes and are responsible for the volume changes observed in astrocytes as well as the shrinkage of the extracellular space associated with intense neuronal activity (105). Finally, another player that helps to actively counteract the increase of $[K^+]_e$ is the Na^+-K^+-$2Cl^-$ co-transporter (60, 148).

Extracellular potassium fluctuates with burst firing. Potassium contributes to the generation of rhythmic oscillations. Indeed, using neonatal rat spinal cord in vitro preparation, Bracci et al. (18) showed that artificially rising $[K^+]_e$ from a control value of 4.5 mM to over a threshold of ~8 mM leads to sustained activation of the spinal locomotor network similar to the locomotor rhythm typically induced by serotonine and NMDA. Interestingly, they found that the suprathreshold concentration range required to elicit such sustained rhythmic motor pattern was very narrow (~1 mM), and when rhythmic activity was elicited with further increases (>2 mM over threshold), it was present only transiently before switching to tonic firing, then into block. Another interesting point is the facilitative effect they reported of co-applying subthreshold concentration of NMDA and serotonine that allows occurrence of rhythmic motor pattern with subthreshold (6 mM) $[K^+]_e$. Similar results were found in a study carried out by Jensen and Yaari (70) on rat hippocampal slices. The authors reported occurrence of periodic bursting in the CA3 region that spread to the CA1 when the slices were exposed to a saline with elevated potassium (7.5 mM). In a more physiological context, Marchetti et al. (96) reported that $[K^+]_e$, as estimated with ion-sensitive electrode recordings, increases to up to 8 and 6 mM in the spinal cord of rats during fictive locomotion induced by electrical stimulation and NMDA, respectively. In this study, the authors did not indicate whether the increases in $[K^+]_e$ occurred before or after the appearance of fictive locomotion, but in a more recent study, Brocard et al. (19), using ion-sensitive electrode recordings in neonate rat spinal cord, showed that potassium increases from a resting value of 4 mM to ~5 mM before the onset of locomotion-like activity induced pharmacologically (with application of NMA and serotonin) or with electrical stimulation of afferent sensory inputs and further to over 6 mM as the locomotor rhythm progresses. This evidence suggests that, at least, the early changes in $[K^+]_e$ can help the emergence of the rhythmic pattern since they appear before any detected rhythmic activity from the ventral roots, whereas the later $[K^+]_e$ increases could be partly consequential to the ongoing neuronal activity since they seem to be related to the increase in burst amplitude. Three of the studies mentioned above were performed on the same preparation (spinal cord, in vitro); in the study of Bracci et al., $[K^+]_e$ was artificially controlled, whereas in the other two the values of $[K^+]_e$ reported were obtained in more physiological conditions. However, the three studies reported similar values of $[K^+]_e$ correlated to occurrence of rhythmic activity. Extracellular potassium increases were also observed in the lamprey spinal cord during fictive swimming (158). The authors reported a two-component $[K^+]_e$ increase, consisting of phasic increases of $[K^+]_e$ of ~0.2 mM linked to the ventral root discharges on the ipsilateral side surimposed on a slow elevation (varying between 0.08 and 0.40 mM) of the baseline level of $[K^+]_e$ that parallels the initiation of ventral root burst activity. The authors did not clearly state whether the onset of the slow elevation precedes that of the detected rhythmic activity, but their observation that the general form of the $[K^+]_e$ curve closely resembles that of the bursts on the ipsilateral side suggests that the phasic $[K^+]_e$ increases may be a consequence of neuronal activity. Similar results have been reported in the cat ventrolateral medulla in parallel with central respiratory activity in the phrenic nerve (125).

FIGURE 2. **Involvement of astrocytes in the generation of bursts in the masticatory CPG**
A1: neurons of the trigeminal main sensory nucleus (NVsnpr) display a bursting pattern in calcium-free medium. *A2*: in control conditions, NVsnpr neurons fire tonically (*left*). Bath application of BAPTA causes one such neuron to burst (*middle*), and I_{NaP} channel blocker riluzole prevents the BAPTA-induced bursting in this neuron (*right*). *B1*: local application of NMDA leads to a significant decrease in extracellular calcium. *B2*: NMDA-induced bursting in a NVsnpr neuron recorded in whole-cell configuration (*left*) is blocked by bath application of Riluzole (*right*). *C*: electrical stimulation of the sensory trigeminal tract at 40 Hz also induces calcium depletion in the extracellular medium and bursts as seen in an extracellular recording of a NVsnpr neuron. *Inset 1* shows a tonic discharge before calcium drops. *Inset 2* shows a burst activity when extracellular calcium level is below 0.3 mM. *D1*: the astrocytic protein S100β causes extracellular calcium to diminish. *D2*: a NVsnpr neuron discharges rhythmically in presence of S100β (*top*), and S100β-induced bursts are blocked by Riluzole (*bottom*). *E1*: in whole-cell recordings, NMDA causes bursting (*left*) but not in presence of an antibody specifically directed against S100β (*right*). E2: in extracellular recordings, electrical stimulation of the sensory trigeminal tract at 40 Hz elicits bursting in control conditions (*left*) but not in presence of an anti-S100β antibody (*right*). *F*: in whole-cell recordings, NMDA induced rhythmic bursting under control conditions (*left*) but only tonic firing after inactivating a neighboring astrocyte with intracellular dialysis of BAPTA (*middle*). Bursting was restored with an external application of S100β (*right*).

In this case, $[K^+]_e$ started to rise before the discharge of action potentials; thus the authors proposed that the efflux of potassium was produced as a consequence of synaptic transmission. Finally, local transients (between 1 and 2 mM) in $[K^+]_e$ were also seen during cortical slow sleep oscillations and spike-wave seizures (4).

Extracellular potassium likely interacts with the conductances that shape the bursts. Indeed, low concentrations of TEA or increased $[K^+]_e$ have been shown to prolong burst duration and to increase oscillation amplitude in the supraoptic nucleus of rats (86) probably by preventing burst termination. A computational model of Hb9 cells suggests that increase in $[K^+]_e$ does not upregulate I_{NaP} in locomotor CPG circuits (19). However, recordings from CA1 pyramidal neurons in hippocampal slices revealed a TTX-sensitive persistent inward current in these neurons that was reversibly enhanced when $[K^+]_e$ was raised (141). It has also been shown that elevated $[K^+]_e$ increases the conductance of the channels mediating I_h (143).

Evidence for spatial buffering of potassium during bursting. Is there any evidence that the astrocyte-driven spatial buffering of potassium takes place along with rhythmic firing in physiological conditions? Working on brain stem slice preparations of neonatal rats, Schnell et al. (137) reported periodic fluctuations of the membrane current of astrocytes occurring in phase with the rhythmic discharges of PBC neurons. Blockade of Kir channels with barium (Ba^{2+}) decreased the amplitude of the periodic membrane current fluctuations by >50%, suggesting that these currents partially reflect the periodic uptake of the elevated extracellular potassium around the astrocytes with each fired burst. Such potassium buffering seems to occur along with large-scale oscillations as well. In the cerebral cortex of anesthetized cats, a periodic increase in intraglial K^+ concentrations ($[K^+]_i$) occurs simultaneously to the depolarizing phase of the slow oscillations (3).

Impairment of spatial buffering may be involved in pathologies like epilepsy. Epilepsy is characterized by periodic seizures resulting from abnormal neuronal hyperexcitability and high synchronicity. Epileptiform activity is generally initiated in restricted areas of the brain but can spread to other parts (8, 106, 121, 151). It has been known for more than four decades that extracellular potassium increases during epileptogenesis (99), and much evidence suggests a role for astrocytes in $[K^+]_e$ regulation in this pathology. For instance, a study by Kivi et al. (75) suggests an impairment of potassium buffering in hippocampal CA1 slices from epileptic rats. Indeed, an application of Ba^{2+} did not affect the level of extracellular potassium in epileptic slices with Ammon' Horn sclerosis. In sclerotic tissues, astrocytes show lower densities of Kir channels (62). Beside Kir channels, many investigations also suggest that astrocyte-expressed aquaporins may play a significant part since they are responsible for the water flow and therefore volume changes in the extracellular space and ultimately the $[K^+]_e$. Indeed, epilepsy has been associated with abnormal expression of aquaporin AQP4 in mice hippocampus (85) and human cortex (97).

Calcium

Astrocytes and calcium homeostasis. Neuronal activity is associated with a decrease of the extracellular concentration of $[Ca^{2+}]_e$ that occurs in parallel to the rise in $[Ca^{2+}]_i$ due to calcium influx into the cells through voltage- and ligand-gated ion channels. Contrary to potassium, much less is known about the role of glia in the regulation of $[Ca^{2+}]_e$. It is, however, known that, in many brain areas, astrocytes possess voltage-gated calcium channels (25, 82) and express calcium sensors (24). Furthermore, direct evidence shows that astrocytes can effectively sense the level of calcium in the extracellular compartment. Indeed, Zanotti and Charles (163) have shown that astrocytes exposed to low $[Ca^{2+}]_e$ respond with increases in $[Ca^{2+}]_i$ that propagate intercellularly as Ca^{2+} waves. This is consistent with the observation that decreased $[Ca^{2+}]_e$ promotes the opening of hemichannels that mediate electrical coupling of neurons and glial cells (150). This low calcium-mediated intracellular calcium rise, however, relies on a release of calcium from intracellular stores since it is inhibited by thapsigargin (163). There is evidence that the astrocytic Ca^{2+} waves modulate the firing frequency of ganglion cells in dissected eyecup retina neurons (108). Lian and Stringer (87) have shown that, during induced spreading depression in the rat cortex, the $[Ca^{2+}]_e$ remained low for a longer time-lapse than normal and that the shape of the recovery curve was altered when astrocytes activity was artificially inhibited with fluorocitrate (FC) and fluoroacetate (FA). Indeed, under control conditions, the $[Ca^{2+}]_e$ recovery curve presents a phase of transient overshoot indicative of an active extrusion of calcium from cells in an amount greater than that which had moved into the cells. The overshoot phase was lacking with the use of FC/FA, suggesting that the failure of astrocytes to actively extrude calcium may account for the longer time required to restore the level of extracellular calcium.

Extracellular calcium fluctuates with burst firing. The extracellular concentration of calcium also seems to be a determinant for bursting in a number of brain areas. Although increases in $[Ca^{2+}]_e$ can lead to bursting as shown by Formenti

et al. (46) in rat thalamic neurons, bursting is most often associated with decreases of $[Ca^{2+}]_e$. In vivo, bursting in the neocortex during seizures is associated with decreases in $[Ca^{2+}]_e$ that occur before the onset of phasic activity (59). In vitro, artificial reduction of $[Ca^{2+}]_e$ has been associated with neuronal bursting in preparations of the rat supraoptic nucleus (86), hippocampus (146), medullary respiratory neurons (36, 73, 114), spinal neurons (19), and neurons of the trigeminal main sensory nucleus (NVsnpr) (FIGURE 2A1) (20, 101, 152). In most of these studies, the medium used was calcium free. In the trigeminal main sensory nucleus, even locally restricted changes induced by extracellular application of the Ca^{2+} chelator BAPTA convert tonic firing into rhythmic bursting (FIGURE 2A2). More interestingly, stimuli like NMDA (locally applied) or stimulation of sensory inputs to the nucleus, which efficiently elicit bursting in these neurons (FIGURE 2, B2, C, AND E2) are also associated with a decrease in $[Ca^{2+}]_e$ (close to 0.89 and 1.1 mM, respectively) (FIGURE 2, B1 AND C). In the spinal cord, Brocard et al. (19) reported 1.03 mM as the extracellular Ca^{2+} concentration below which they observed locomotor-like activity when they electrically stimulated the ventral funiculus, whereas in the main sensory trigeminal nucleus the $[Ca^{2+}]_e$ needed to drop beneath 0.4 mM for rhythmic activity to appear (101). These differences may reflect differences in age, structure, or electrode placement between these two studies. In neurons of the trigeminal main sensory nucleus, bursting elicited by NMDA or BAPTA applications is driven by I_{NaP} (FIGURE 2A2 AND 2B2). Depletion of extracellular calcium shifts the *I*-V curve of I_{NaP} toward more hyperpolarized potentials (86, 101, 149), and from predictions based on a computational model of Hb9 cells, it appears that a slight shift of I_{NaP} activation suffices to switch the neuron firing pattern from tonic to rhythmic bursting (19). The work by Armstrong (5) in the squid giant axon suggests that Ca^{2+} may favor closing of the channel by occupying its pore. In its absence, closing slows considerably or does not occur. This effect of calcium may also help understand the voltage dependency of the activation range of I_{NaP} since the ability of calcium to enter the pore and block it is reduced as voltage is driven negative.

Unlike sodium-persistent channels, activation of LVA Ca^{2+} channels is promoted with rises in $[Ca^{2+}]_e$. This effect may result from the fact that these channels are activated at more hyperpolarized potentials. Increases of $[Ca^{2+}]_e$ hyperpolarize thalamic neurons and shift the conductance-voltage relationship of their LVA Ca^{2+} channels to the right (46). The hyperpolarization, which may result from a masking of the negative fixed charges on the membrane surface by the calcium ions facilitates activation of the LVA channels, whereas the increased Ca^{2+} driving force favors appearance of low-threshold Ca^{2+} spikes and eventually bursting.

Astrocyte-mediated extracellular calcium depletions during bursting. Although often postulated, direct evidence of astrocytic regulation of extracellular calcium were only recently obtained. We recently showed that an astrocytic protein, S100β, reduces $[Ca^{2+}]_e$ (FIGURE 2D1) and induces I_{NaP}-driven bursting in neurons of the trigeminal main sensory nucleus (FIGURE 2D2) (101). Protein S100β was proven to be released from astrocytes (155) after elevation of cytosolic Ca^{2+} (33), but the exact mechanisms underlying its release or secretion have not been deciphered yet. Some studies (26, 134) suggested that these mechanisms may involve the activation of glutamate mGluR3 and/or A1 adenosine receptors, whereas others (134) have ruled out involvement of Cx43 hemichannels. S100β exerts many actions, one of which is calcium chelation (94, 95). In support of this role, we have observed that blockade of endogenous S100β with application of an antibody directed against it prevents bursting and Ca^{2+} decreases induced in the trigeminal sensory nucleus with NMDA or sensory fibers stimulation (FIGURE 2, E1 AND E2; Ref. 101). These findings strongly suggest a prominent role for astrocytes in rhythmogenesis. This is further supported by the finding that preventing activation of astrocytes with intracellular dialysis of BAPTA in one of several connected astrocytes led to cessation of NMDA-induced bursting (FIGURE 2F; Ref. 101) in adjacent neurons. Bursting blocked by this procedure could be restored by exogenous application of S100β (FIGURE 2F, RIGHT; Ref. 101). Thus we propose that in the trigeminal main sensory nucleus, which is postulated to form part of the core of the masticatory CPG, rhythmic activity results from activation of astrocytes by incoming sensory glutamatergic inputs (101), leading to release of S100β, which in turn binds extracellular calcium, causing a decrease in $[Ca^{2+}]_e$ and a consequent shift in I_{NaP} activation curve, which facilitates bursting (see FIGURE 4). This study constitutes the first demonstration that directly links astrocytic S100β to neuronal firing pattern in individual cells (101). However, other evidence suggests that S100β can also play a role in large-scale oscillations. In two studies using S100β knockout mice, no significant differences were found in the spontaneous oscillations detected in the hippocampus and the neocortex compared with wild-type mice (133, 134). However, these oscillations diverged during kainate-induced seizures. Under these conditions, there was a significant increase in the amplitude of gamma waves (133, 134) that was correlated with increased level of extracellular S100β in the wild-type mice

(134), suggesting that S100β may contribute to gamma oscillations in the hippocampus. Gamma oscillations are high-frequency waves (30–80 Hz) associated with attentive behavioral states that can be found in the neocortex and the hippocampus. Evidence of S100β implication in these rhythmic events support our data showing an important role for S100β in rhythmogenesis in the masticatory GPG.

Several other findings link changes in astrocytic functions to dysregulation of extracellular calcium and brain pathologies. In kainate-induced epilepsy in rats, for instance, immunocytochemical investigations have shown an upregulation of L-type voltage-gated calcium channel α2 subunit in astrocytes surrounding the lesion (160). No significant changes were reported in neurons. In the hippocampi of patients who suffered from temporal lobe epilepsy associated with Ammon's horn sclerosis, astrocytes were also strongly immunoreactive for α1c subunits (42). Some of the voltage-gated calcium channels have a relatively high threshold of activation, and, given the very negative membrane potential of healthy astrocytes, it is unlikely that they can be depolarized enough to activate these channels. Nevertheless, it has been shown using brain slices or cultures that astrocytes from human sclerotic epileptogenic hippocampal seizure foci display more depolarized membrane potential (around −55 mV) compared with astrocytes from nonsclerotic tissue (around −75 to −80 mV) (112) and express higher TTX-sensitive Na^+ channel density, allowing them to generate action potential-like responses with membrane depolarization (17, 112). In these conditions, one should expect such upregulations of L-type voltage-gated calcium channel subunits to lead to an increased flow of calcium into astrocytes, potentially causing a decrease in $[Ca^{2+}]_e$. Parkinson's disease may be another example of pathology that results from an inefficient regulation of calcium levels in the extracellular space. Symptoms of Parkinson's disease include neuronal death and excessive synchronicity of beta waves in the cortex and in the basal ganglia (22, 56, 153). Glial cells play a significant role in the ontogenesis of that disease (55). In a mouse model of MPTP (1-methyl-4-phenyl-1,2,3,6-tetrahydropyridine)-induced Parkinson's disease, the number of S100β-positive astrocytes increases in the striatum and the substantia nigra immediately after treatment with MPTP but declines after 7 days (104). Increases in the levels of S100β were also reported in midbrain slices and cerebrospinal fluid of patients who suffered from Parkinson's disease (135). S100β is a calcium-binding protein (94, 95), and it is possible that its transitory accumulation in the extracellular space leads to a chelation of calcium. A precursor sign of Parkinson's disease could then be a transient decrease of calcium in the extracellular space.

Sodium

Astrocytes and sodium homeostasis. As neurons fire, there is a decrease in the extracellular sodium concentration ($[Na^+]_e$) due to influx of sodium ions into the cells through voltage- and ligand-gated ion channels (41). Indeed, in a study carried out on hippocampal slices, Karus et al. (74) reported that, during bursts, the neuronal intracellular concentration of sodium ($[Na^+]_i$) increases to up to 22 mM from a resting baseline value of ~14 mM and recovers to around baseline level between bursts. Intraneuronal concentrations of sodium need to be tightly controlled to maintain cell integrity and excitability and also because extrusion of sodium ions by the Na^+-K^+-ATPase is an energy-expensive process. How do astrocytes participate in sodium homeostasis? Astrocytes express voltage-gated Na^+ channels (for a review about sodium homeostasis and signaling in astrocytes, see Ref. 128), which allows for a small but steady influx of Na^+ ions to ensure the maintenance of cytoplasmic Na^+ at concentrations required for proper functioning of the glial Na^+-K^+ pump (142). Moreover, sodium signaling concomitant with neuronal activity has been shown to occur in astrocytes. Indeed, combining somatic whole-cell patch-clamp recordings with quantitative sodium imaging with the sodium-sensitive fluorescent indicator dye (sodium-binding benzofuran isophthalate), Bennay et al. (15) showed that short bursts of synaptic activity resulted in glial sodium signals of up to 9 mM in cellular branches of cerebellar Bergmann glial cells. These sodium increases persisted for tens of seconds. Sodium may also build up in astrocytes following excitatory neuronal activity because of the glial glutamate transporter, which carries three Na^+ ions with each glutamate molecule (80). In cultures of cortical astrocytes, uptake of glutamate produces intercellular sodium waves that occur in parallel with calcium waves following stimulation of a single astrocyte. Sodium underlying these waves has to come from the extracellular space since it could not be released from the intracellular stores as with calcium. Thus, at sites of intense activity, the consequent lowering of extracellular sodium could weaken the drive for this ion toward the neuronal intracellular compartment. Other than the glutamate transporter, the glial Na^+-K^+ pump, which is involved in $[K^+]_e$ homeostasis, can also greatly impact neuronal sodium homeostasis. Indeed, blocking astrocyte metabolism during basal activity using sodium-fluoroacetate results in an increase of baseline intracellular sodium of ~4 mM in hippocampal neurons and by ~12 mM in astrocytes (74). The authors attribute

the larger increase in astrocytes to the weakening of the glial Na^+-K^+-ATPase. Under conditions of increased network activity, blocking of astrocyte metabolism increases even more the baseline intracellular sodium in both cells types but also produces a nearly fivefold prolongation of individual epileptiform bursts and similar increase in the number of population spikes per burst (74). The authors proposed that the increased neuronal excitability results, in part, from reduced glutamate uptake due to reduced activity of the glutamate transporter that greatly depends on the transmembrane sodium gradient in astrocytes, which in turn depends on the activity of the Na^+-K^+-ATPase. Furthermore, since the glial Na^+-K^+-ATPase is also involved in the clearance of extracellular potassium following intense neuronal activity, its weakening reduces potassium intake, thus increasing neuronal excitability. No measurements of extracellular sodium have been made in parallel in this study; however, this evidence of astrocyte involvement in the control of neuronal $[Na^+]_i$ suggests that, even indirectly, by achieving other basic cellular functions, astrocytes may participate in the homeostasis of extracellular sodium.

Extracellular sodium and bursting. Studies addressing the direct role of sodium ions in bursting are relatively scarce. Many of the studies addressed the involvement of sodium channels rather than the role of the ionic sodium gradient per se. One study by Li and Hatton (86) carried out on the magnocellular neurons of the hypothalamic supraoptic nucleus (SON) showed that both $[Na^+]_e$ and $[Na^+]_i$ are determinants for the low calcium-mediated burst firing observed in a subpopulation of these neurons. They examined the effect of reducing the extracellular sodium and reported that this treatment abolished or reduced bursting in all tested cells. Finally, even though no study has formally measured the changes in extracellular sodium during rhythmic activities, $[Na^+]_e$ is likely to decrease because of all the voltage- and ligand-activated channels allowing movements of Na^+ ions from the extracellular space toward the intracellular compartment. However, the question remains as to the extent of sodium depletion and how such decreases may influence other conductances involved in bursting.

Evidence for synchronized sodium signaling in astrocytes somata during bursting. In the study cited above, Karus et al. (74) showed that, during neuronal recurrent bursting, astrocytes showed an increase of ~2.9 mM in $[Na^+]_i$ that occurred in parallel with the transient $[Na^+]_i$ increase seen in neurons. In ~30% of the astrocytes, this increase was followed by an undershoot below baseline. The increases of astrocytic $[Na^+]_i$ observed during neuronal bursts were accompanied by recurring membrane depolarizations of ~10 mV and were paralleled by recurring transient increases of $[K^+]_e$ of up to 2 mM. Between bursts, the astrocytic $[Na^+]_i$ recovered to resting baseline values. Using several pharmacological tools, the authors concluded that sodium signals in astrocytes result from dual contribution of two opposing mechanisms: an influx of sodium ions caused by the sodium-dependent glutamate uptake and an efflux of sodium ions brought out by the elevated $[K^+]_e$-induced activation of the Na^+-K^+-ATPase.

Chloride

The movements of chloride ions in response to neuronal activation are more complex than the other ions (41). Probably, since it is the main permeable anion, chloride ion movements are partly determined by balancing measures in relation to

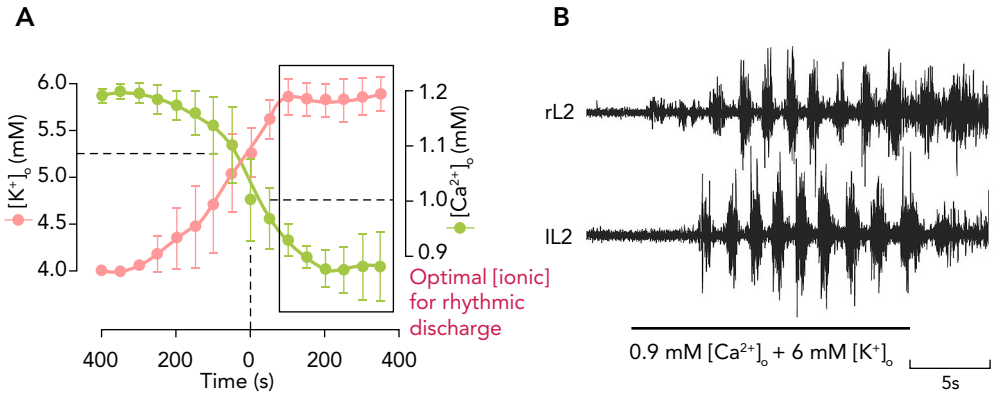

FIGURE 3. **Example of synergistic interactions between potassium and calcium in rhythmogenesis**
A: evolution of extracellular concentration of calcium (green) and potassium (pink) before and after the onset (at 0 ms) of a locomotor-like bursting episode. Optimal concentrations of calcium and potassium for a bursting activity are emphasized by the rectangle. A rhythmic activity appears at concentrations of calcium and potassium close to 0.9 and 6 mM, respectively. *B*: extracellular recordings in the right and left L2 segments (rL2 and lL2) of rat spinal cord along with application of 0.9 mM $[Ca^{2+}]_e$ and 6 mM $[K^+]_e$. **Figure** was modified from Ref. 19 with permission.

fluctuations of the cation gradient concentration. Dietzel et al. (41) reported that, during stimulus-induced self-sustained afterdischarges (SAD) in neurons of the sensorimotor cortex of cats, $[Cl^-]_e$ always showed an average increase of 7 mM (when measured at a depth of 1 mm), often preceded by an initial small decrease. They observed that the maximum increase appears to coincide with the end of the ictal period.

Astrocytes and chloride homeostasis. Chloride channels exist in astrocytes and include volume-sensitive chloride channels (157). The latter participate

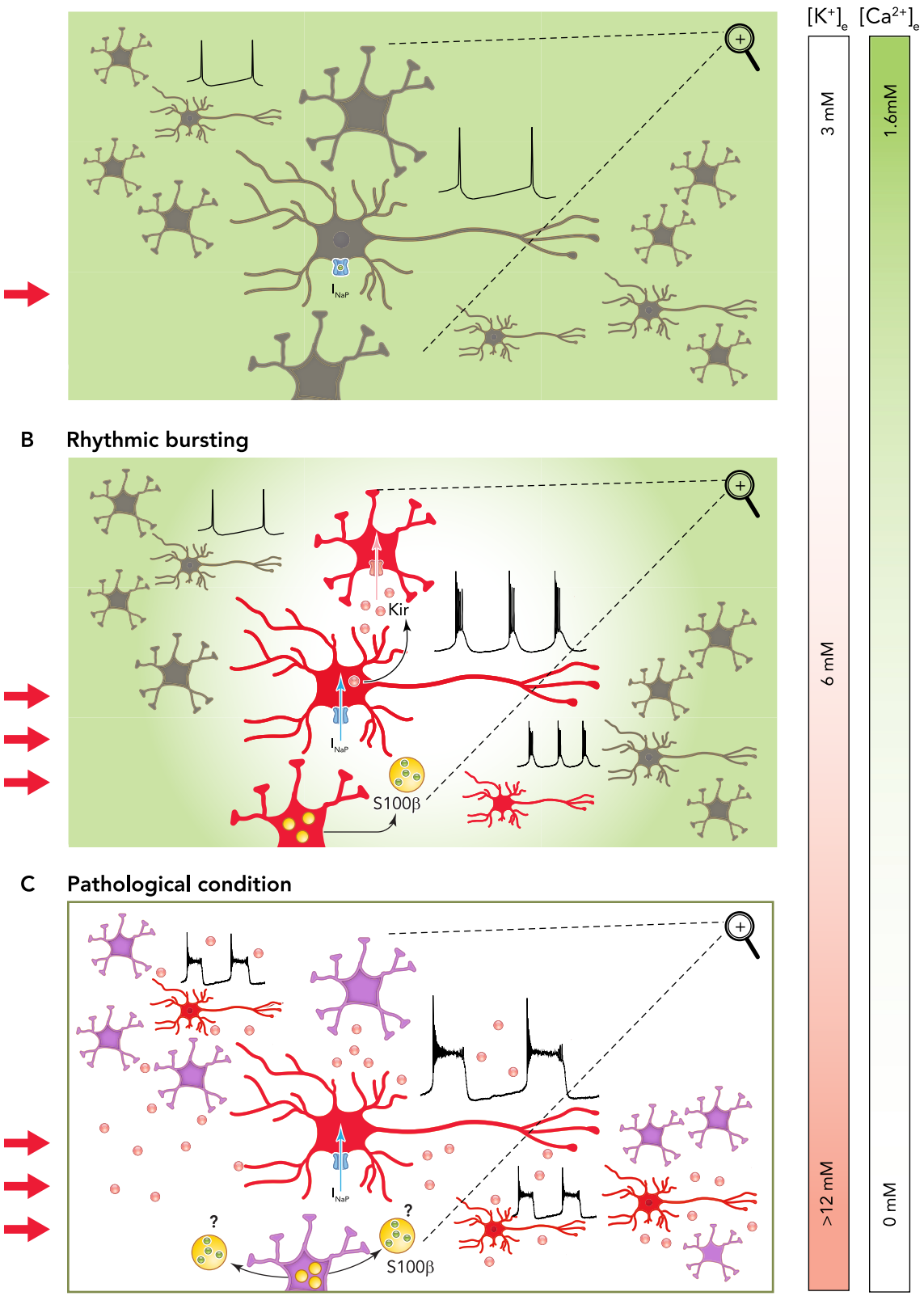

in ion homeostasis mainly through the process of astrocyte swelling (30). By swelling, astrocytes change their volume and thereby control the concentration of several ions in both the intra- and extracellular space. In addition to potassium-mediated machinery, which intervenes in astrocyte swelling (39, 107), an inward rectifier chloride current (14, 81) and Na^+-K^+-Cl^- cotransporter are also activated (69). The participation of chloride channels to astrocytic volume change might result from their association with actin proteins, which form the cytoskeleton (157). Bikson and collaborators (16) tested the effect of DNDS (4,4′-dinitrostilbene-2,2′-disulfonic acid), a glial Cl^- channel blocker (103), on the duration of low calcium-mediated bursts in rat pyramidal CA1 cells and found that high concentration of DNDS caused a 6- to 10-fold increase in burst duration, suggesting that glial uptake of chloride ions contributes to the burst termination.

Extracellular chloride and bursting. Working on the leech's Retzius neurons, Beck and colleagues found that decreasing $[Cl^-]_e$ (≤1 mM) induces a sustained membrane depolarization and recurrent bursting activity that were accompanied by recurrent rises in intracellular Ca^{2+}, which oscillated in synchrony with the bursts. Using a chloride-free and calcium-free medium, they determined that the intracellular calcium rises were presumably due to Ca^{2+} influx through voltage-dependent Ca^{2+} channels, since they could no longer be seen in this medium. Moreover, the bursting activity was not affected by depletion of intracellular calcium but was inhibited by saxitoxin, a sodium channel blocker, suggesting that it relies on I_{NaP} (13). In rat hippocampal slices, spontaneous (63) or stimulus-evoked (9) bursting discharges also developed when the $[Cl^-]_e$ was decreased. These cellular discharges were accompanied for a time with synchronous oscillations in the field potential. However, longer exposure to low chloride medium desynchronized the firing activity of neuronal populations in the CA1 region of hippocampal slices, which may explain the anti-epileptic effect of chloride-cotransport blockade by furosemide (64). Reciprocally, it has been shown that calcium-free mediated bursting occurs concomitantly with large decreases in $[Cl^-]_e$ (58).

Synergistic Interactions and Rhythmogenesis

Changes in the ionic gradient concentration of the main ions that regulate brain activity exert tremendous effects on neuronal excitability and are determinant of the neuronal firing mode. By their concerted actions on the rhythmogenic conductances, they may act in synergy to promote rhythmogenesis. Indeed, Brocard et al. (19) reported that such a synergistic effect exists between the $[Ca^{2+}]_e$ reduction and the $[K^+]_e$ increase for burst generation in the locomotor CPG (FIGURE 3). The authors stated that both $[Ca^{2+}]_e$ and $[K^+]_e$ concurrently changed before any rhythmic activity was detected from ventral roots, suggesting that these changes are not just a consequence of the neuronal activity but are part of the cause for the rhythmic pattern observed. They confirmed this synergistic interaction by artificially manipulating both ion concentrations while recording neuronal activity and reported that concomitant reduction of $[Ca^{2+}]_e$ to 0.9 mM and increase of $[K^+]_e$ to 6 mM (the same values reported with physiologically induced changes in concentration for both ions) elicited bursts in 25% of the recorded neurons. A similar interaction between both ion concentrations reported this time as a "Ca^{2+}/K^+ antagonism" is also encountered in mice rhythmogenic inspiratory active pre-Bötzinger complex (117). The authors indeed showed that the rhythm generated in 3 mM K^+ and 1 mM Ca^{2+} is depressed following a modest rise of Ca^{2+} and restored when K^+ is subsequently raised. Ultimately, they proposed that the optimal window to obtain long-term stable slice rhythm would be 0.75–1 mM for calcium and 4–6 mM for potassium, which seems to be in accordance with the values obtained for either ion in more physiological conditions (4, 19, 96, 125).

How do all of the elements converge to allow the emergence of an oscillatory activity? From the reports examined here, it seems that the starting point is the increased firing that causes an elevation of extracellular potassium. According to Hounsgaard and Nicholson (65), an individual burst is initiated when intense neuronal firing results in a local increase in $[K^+]_e$ that would in turn depolarize neighboring neurons. Increased activity

FIGURE 4. **A general model for rhythmogenesis in CPGs**
A: under resting conditions, glutamatergic inputs are low (red arrow), astrocytes (gray) are at resting activity levels, $[Ca^{2+}]_e$ (green) is elevated, and $[K^+]_e$ (pink) is low. The I_{NaP} channels are obstructed by calcium (green dot), and neurons fire tonically. *B*: as the glutamatergic inputs increase, $[K^+]_e$ (pink dots) rises, and astrocytes get activated (red), release S100β (yellow), and initiate spatial buffering through Kir channels. Protein S100β chelates calcium and causes $[Ca^{2+}]_e$ to drop. As a consequence, I_{NaP} channels are freed and drive bursting in neurons (red). The bursting population is limited to the extent of coupled astrocytes forming a syncytium. *C*: under pathological conditions, astrocytes (purple) fail to initiate spatial buffering in the presence of intense neuronal activity, leading to an accumulation of potassium and a spread of excitation and depolarization block among neurons. The level of S100β in the extracellular space may increase and further lead to neuronal hyperexcitability by decreasing $[Ca^{2+}]_e$.

of these neighboring neurons would boost the $[K^+]_e$ to a further extent. This increased activity and $[K^+]_e$ would directly activate the astrocytes and cause them to start the spatial buffering of potassium to prevent local build-up of extracellular K^+ that would cause a depolarizing block and cessation of cell activity. Spread of K^+ will be limited only to astrocytes that are coupled. Thus gap-junctional coupling between astrocytes may provide a means to limit spreading of activity to a specific neuronal population as well as an explanation for the observed synergistic interaction between ions. As already stated, extracellular accumulation of K^+ increases gap-junctional coupling between astrocytes. Interestingly, Scemes and Spray (136) found that this increase in dye-coupling long outlasted the exposure to elevated potassium, suggesting that the effect of potassium on coupling may be indirect. Indeed, the elevated extracellular K^+ causes astrocytic membrane depolarization and leads to the influx of Ca^{2+} through L-type voltage-activated Ca^{2+} channels (34, 43, 147), promoting increases in $[Ca^{2+}]_i$. Blocking the influx of calcium with the L-type calcium channel blocker nifedipine or potentiating this influx with Bay-K-8644 prevented and potentiated, respectively, the K^+-induced increase in coupling (34). At last, they provide evidence that the K^+-induced increased coupling relies on the activation of a CaM kinase by the intracellular calcium rise since it can be prevented by the calmodulin antagonist calmidazolium and by the inhibitor of CaM kinases KN-93. The authors hypothesized that the increased coupling might result from an increased number of active channels within gap-junction plaques. However, only very large increases of extracellular potassium (50 mM), much larger than those observed even with intense neuronal activity of 8–12 mM (140), yielded an elevation of $[Ca^{2+}]_i$ in astrocytes, suggesting that voltage-gated Ca^{2+} influx would be unique to pathological conditions associated with deregulations of $[K^+]_e$. However, the accumulation of sodium in astrocytes during intense excitatory discharge may also cause a calcium entry by reversing the function of the sodium/calcium exchanger (52, 124, 127) and consequently lead to an extracellular decrease of Ca^{2+}. Other mechanisms may also account for the decreased calcium level in the extracellular compartment that occurs in conjunction with rhythmic firing. Astrocytes have a wide array of ionotropic and metabotropic receptors (25), the activation of which leads to intracellular rises of calcium, and glutamate-induced calcium waves in astrocytes have been commonly reported (1). As described above, data from our laboratory suggest that glutamatergic activation of astrocytes may also cause release of the protein S100β from astrocytes, leading to extracellular calcium depletion, subsequent I_{NaP} activation, and burst firing (101). FIGURE 4 summarizes how astrocytes may participate in emergence and synchronization of rhythmic firing in NVsnpr neurons. The proposed model rests on the fact that NVsnpr astrocytes are activated by glutamatergic afferent inputs to this nucleus, but only if they reach a sufficient level of activity. At high activity level, glutamate or K^+ released from these inputs activate astrocytes and cause release of S100β. The extent of neurons exposed to the released S100β will depend on the extent of coupled astrocytes. Among these neurons, only those having I_{NaP} will change their firing. In young rats (P8-12), only 38% of the dorsal NVsnpr neurons perfused with a calcium-free medium showed bursts firing, and bursting and non-bursting cells displayed distinct morphological characteristics and significantly different input resistance and membrane capacitance (152). However, using older rats (P16), Brocard et al. showed that 85% of dorsal NVsnpr neurons had intrinsic bursting properties in calcium-free medium and that bursting relied on I_{NaP} in all tested cells (20). We postulate that the extent of the active network would likely be determined by the population of cells (neurons and astrocytes) that share the same input, and since the primary afferent inputs are somatotopically organized, only functionally related cells would share the same input. Eventually, cessation of primary afferent activation would stop the network activation or excessive stimulation would depolarize the neurons beyond the range of I_{NaP} activation.

Conclusions

The classic concept in which brain function relied exclusively on neuron-to-neuron communication was shattered by evidence in which glial cells switched from the role of brain glue to active information processors expressing a large spectrum of ion channels and receptors. This review recounts the progress made in understanding the prominent role that glial cells play in the generation and maintenance of rhythmic oscillations. Glial cells have proven to be essential partners in coordinating the numerous elements participating in rhythmogenesis through a cross-talk with surrounding neurons. The control of extracellular concentration of ions necessary for rhythmic activities to occur clearly depicts that dialogue. ■

This work was supported by grants from the Canadian Institutes for Health Research and the Network for Oral and Bone Health Research (RSBO), and we are grateful to the Groupe de Recherche sur le Système Nerveux Central (GRSNC) for infrastructural support.

No conflicts of interest, financial or otherwise, are declared by the author(s).

Author contributions: A. Kadala and A. Kolta drafted manuscript; A. Kadala, D.V., P.M., and A. Kolta edited and revised manuscript; A. Kadala, D.V., P.M., and A. Kolta approved final version of manuscript; D.V. and P.M. prepared figures.

References

1. Agulhon C, Petravicz J, McMullen AB, Sweger EJ, Minton SK, Taves SR, Casper KB, Fiacco TA, McCarthy KD. What is the role of astrocyte calcium in neurophysiology? *Neuron* 59: 932–946, 2008.
2. Alzheimer C, Schwindt PC, Crill WE. Modal gating of Na^+ channels as a mechanism of persistent Na^+ current in pyramidal neurons from rat and cat sensorimotor cortex. *J Neurosci* 13: 660–673, 1993.
3. Amzica F, Massimini M, Manfridi A. Spatial buffering during slow and paroxysmal sleep oscillations in cortical networks of glial cells in vivo. *J Neurosci* 22: 1042–1053, 2002.
4. Amzica F, Steriade M. Neuronal and glial membrane potentials during sleep and paroxysmal oscillations in the neocortex. *J Neurosci* 20: 6648–6665, 2000.
5. Armstrong CM. Distinguishing surface effects of calcium ion from pore-occupancy effects in Na^+ channels. *Proc Natl Acad Sci USA* 96: 4158–4163, 1999.
6. Armstrong CM, Matteson DR. Two distinct populations of calcium channels in a clonal line of pituitary cells. *Science* 227: 65–67, 1985.
7. Astori S, Wimmer RD, Prosser HM, Corti C, Corsi M, Liaudet N, Volterra A, Franken P, Adelman JP, Luthi A. The Ca(V)3.3 calcium channel is the major sleep spindle pacemaker in thalamus. *Proc Natl Acad Sci USA* 108: 13823–13828, 2011.
8. Avoli M, D'Antuono M, Louvel J, Kohling R, Biagini G, Pumain R, D'Arcangelo G, Tancredi V. Network and pharmacological mechanisms leading to epileptiform synchronization in the limbic system in vitro. *Prog Neurobiol* 68: 167–207, 2002.
9. Avoli M, Drapeau C, Perreault P, Louvel J, Pumain R. Epileptiform activity induced by low chloride medium in the CA1 subfield of the hippocampal slice. *J Neurophysiol* 64: 1747–1757, 1990.
10. Bal T, McCormick DA. Mechanisms of oscillatory activity in guinea-pig nucleus reticularis thalami in vitro: a mammalian pacemaker. *J Physiol* 468: 669–691, 1993.
11. Barres BA, Chun LL, Corey DP. Ion channels in vertebrate glia. *Ann Rev Neurosci* 13: 441–474, 1990.
12. Bean BP. Two kinds of calcium channels in canine atrial cells. Differences in kinetics, selectivity, and pharmacology. *J Gen Physiol* 86: 1–30, 1985.
13. Beck A, Lohr C, Nett W, Deitmer JW. Bursting activity in leech Retzius neurons induced by low external chloride. *Pflügers Arch* 442: 263–272, 2001.
14. Benesova J, Rusnakova V, Honsa P, Pivonkova H, Dzamba D, Kubista M, Anderova M. Distinct expression/function of potassium and chloride channels contributes to the diverse volume regulation in cortical astrocytes of GFAP/EGFP mice. *PLos One* 7: e29725, 2012.
15. Bennay M, Langer J, Meier SD, Kafitz KW, Rose CR. Sodium signals in cerebellar Purkinje neurons and Bergmann glial cells evoked by glutamatergic synaptic transmission. *Glia* 56: 1138–1149, 2008.
16. Bikson M, Ghai RS, Baraban SC, Durand DM. Modulation of burst frequency, duration, and amplitude in the zero-Ca^{2+} model of epileptiform activity. *J Neurophysiol* 82: 2262–2270, 1999.
17. Bordey A, Sontheimer H. Properties of human glial cells associated with epileptic seizure foci. *Epilepsy Res* 32: 286–303, 1998.
18. Bracci E, Beato M, Nistri A. Extracellular K^+ induces locomotor-like patterns in the rat spinal cord in vitro: comparison with NMDA or 5-HT induced activity. *J Neurophysiol* 79: 2643–2652, 1998.
19. Brocard F, Shevtsova NA, Bouhadfane M, Tazerart S, Heinemann U, Rybak IA, Vinay L. Activity-dependent changes in extracellular Ca^{2+} and K^+ reveal pacemakers in the spinal locomotor-related network. *Neuron* 77: 1047–1054, 2013.
20. Brocard F, Verdier D, Arsenault I, Lund JP, Kolta A. Emergence of intrinsic bursting in trigeminal sensory neurons parallels the acquisition of mastication in weanling rats. *J Neurophysiol* 96: 2410–2424, 2006.
21. Brown AM, Schwindt PC, Crill WE. Different voltage dependence of transient and persistent Na^+ currents is compatible with modal-gating hypothesis for sodium channels. *J Neurophysiol* 71: 2562–2565, 1994.
22. Brown P. Abnormal oscillatory synchronisation in the motor system leads to impaired movement. *Curr Opin Neurobiol* 17: 656–664, 2007.
23. Brumberg JC, Nowak LG, McCormick DA. Ionic mechanisms underlying repetitive high-frequency burst firing in supragranular cortical neurons. *J Neurosci* 20: 4829–4843, 2000.
24. Chattopadhyay N, Evliyaoglu C, Heese O, Carroll R, Sanders J, Black P, Brown EM. Regulation of secretion of PTHrP by Ca^{2+}-sensing receptor in human astrocytes, astrocytomas, and meningiomas. *Am J Physiol Cell Physiol* 279: C691–C699, 2000.
25. Christensen RK, Petersen AV, Perrier JF. How do glial cells contribute to motor control? *Curr Pharmaceutical Design* 19: 4385–4399, 2013.
26. Ciccarelli R, Di Iorio P, Bruno V, Battaglia G, D'Alimonte I, D'Onofrio M, Nicoletti F, Caciagli F. Activation of A(1) adenosine or mGlu3 metabotropic glutamate receptors enhances the release of nerve growth factor and S-100beta protein from cultured astrocytes. *Glia* 27: 275–281, 1999.
27. Cobb SR, Larkman PM, Bulters DO, Oliver L, Gill CH, Davies CH. Activation of Ih is necessary for patterning of mGluR and mAChR induced network activity in the hippocampal CA3 region. *Neuropharmacology* 44: 293–303, 2003.
28. Colombo E, Franceschetti S, Avanzini G, Mantegazza M. Phenytoin inhibits the persistent sodium current in neocortical neurons by modifying its inactivation properties. *PLos One* 8: e55329, 2013.
29. Coombes S, Bressloff PC. *Bursting: The Genesis of Rhythm in the Nervous System*. Hackensack, NJ: World Scientific, 2005, p. 401.
30. Crepel V, Panenka W, Kelly ME, MacVicar BA. Mitogen-activated protein and tyrosine kinases in the activation of astrocyte volume-activated chloride current. *J Neurosci* 18: 1196–1206, 1998.
31. D'Ambrosio R, Gordon DS, Winn HR. Differential role of KIR channel and Na^+/K^+-pump in the regulation of extracellular K^+ in rat hippocampus. *J Neurophysiol* 87: 87–102, 2002.
32. Darbon P, Tscherter A, Yvon C, Streit J. Role of the electrogenic Na/K pump in disinhibition-induced bursting in cultured spinal networks. *J Neurophysiol* 90: 3119–3129, 2003.
33. Davey GE, Murmann P, Heizmann CW. Intracellular Ca^{2+} and Zn^{2+} levels regulate the alternative cell density-dependent secretion of S100B in human glioblastoma cells. *J Biol Chem* 276: 30819–30826, 2001.
34. De Pina-Benabou MH, Srinivas M, Spray DC, Scemes E. Calmodulin kinase pathway mediates the K^+-induced increase in Gap junctional communication between mouse spinal cord astrocytes. *J Neurosci* 21: 6635–6643, 2001.
35. Deitmer JW, Verkhratsky AJ, Lohr C. Calcium signalling in glial cells. *Cell Calcium* 24: 405–416, 1998.
36. Del Negro CA, Koshiya N, Butera RJ Jr, Smith JC. Persistent sodium current, membrane properties and bursting behavior of pre-Botzinger complex inspiratory neurons in vitro. *J Neurophysiol* 88: 2242–2250, 2002.
37. Del Negro CA, Morgado-Valle C, Hayes JA, Mackay DD, Pace RW, Crowder EA, Feldman JL. Sodium and calcium current-mediated pacemaker neurons and respiratory rhythm generation. *J Neurosci* 25: 446–453, 2005.
38. Destexhe A, Contreras D, Steriade M. Spatiotemporal analysis of local field potentials and unit discharges in cat cerebral cortex during natural wake and sleep states. *J Neurosci* 19: 4595–4608, 1999.
39. Dibaj P, Kaiser M, Hirrlinger J, Kirchhoff F. Neusch Kir4 C.1. channels regulate swelling of astroglial processes in experimental spinal cord edema. *J Neurochem* 103: 2620–2628, 2007.

40. Dietzel I, Heinemann U. Dynamic variations of the brain cell microenvironment in relation to neuronal hyperactivity. *Ann NY Acad Sci* 481: 72–86, 1986.

41. Dietzel I, Heinemann U, Hofmeier G, Lux HD. Stimulus-induced changes in extracellular Na^+ and Cl^- concentration in relation to changes in the size of the extracellular space. *Exp Brain Res* 46: 73–84, 1982.

42. Djamshidian A, Grassl R, Seltenhammer M, Czech T, Baumgartner C, Schmidbauer M, Ulrich W, Zimprich F. Altered expression of voltage-dependent calcium channel alpha(1) subunits in temporal lobe epilepsy with Ammon's horn sclerosis. *Neuroscience* 111: 57–69, 2002.

43. Duffy S, MacVicar BA. In vitro ischemia promotes calcium influx and intracellular calcium release in hippocampal astrocytes. *J Neurosci* 16: 71–81, 1996.

44. el Manira A, Tegner J, Grillner S. Calcium-dependent potassium channels play a critical role for burst termination in the locomotor network in lamprey. *J Neurophysiol* 72: 1852–1861, 1994.

45. Enkvist MO, McCarthy KD. Astroglial gap junction communication is increased by treatment with either glutamate or high K^+ concentration. *J Neurochem* 62: 489–495, 1994.

46. Formenti A, De Simoni A, Arrigoni E, Martina M. Changes in extracellular Ca^{2+} can affect the pattern of discharge in rat thalamic neurons. *J Physiol* 535: 33–45, 2001.

47. Forrest MD. Mathematical model of bursting in dissociated purkinje neurons. *PLos One* 8: e68765, 2013.

48. Franceschetti S, Lavazza T, Curia G, Aracri P, Panzica F, Sancini G, Avanzini G, Magistretti J. Na^+-activated K^+ current contributes to postexcitatory hyperpolarization in neocortical intrinsically bursting neurons. *J Neurophysiol* 89: 2101–2111, 2003.

49. Gamba G. Molecular physiology and pathophysiology of electroneutral cation-chloride cotransporters. *Physiol Rev* 85: 423–493, 2005.

50. Ghamari-Langroudi M, Bourque CW. Flufenamic acid blocks depolarizing afterpotentials and phasic firing in rat supraoptic neurones. *J Physiol* 545: 537–542, 2002.

51. Ghazanfar AA, Chandrasekaran C, Logothetis NK. Interactions between the superior temporal sulcus and auditory cortex mediate dynamic face/voice integration in rhesus monkeys. *J Neurosci* 28: 4457–4469, 2008.

52. Goldman WF, Yarowsky PJ, Juhaszova M, Krueger BK, Blaustein MP. Sodium/calcium exchange in rat cortical astrocytes. *J Neurosci* 14: 5834–5843, 1994.

53. Golomb D, Yue C, Yaari Y. Contribution of persistent Na+ current and M-type K^+ current to somatic bursting in CA1 pyramidal cells: combined experimental and modeling study. *J Neurophysiol* 96: 1912–1926, 2006.

54. Guatteo E, Franceschetti S, Bacci A, Avanzini G, Wanke E. A TTX-sensitive conductance underlying burst firing in isolated pyramidal neurons from rat neocortex. *Brain Res* 741: 1–12, 1996.

55. Halliday GM, Stevens CH. Glia: initiators and progressors of pathology in Parkinson's disease. *Movement Disorders* 26: 6–17, 2011.

56. Hammond C, Bergman H, Brown P. Pathological synchronization in Parkinson's disease: networks, models and treatments. *Trends Neurosci* 30: 357–364, 2007.

57. Harris-Warrick RM. General principles of rhythmogenesis in central pattern generator networks. *Prog Brain Res* 187: 213–222, 2010.

58. Heinemann U, Albrecht D, Kohr G, Rausche G, Stabel J, Wisskirchen T. Low-Ca^{2+}-induced epileptiform activity in rat hippocampal slices. *Epilepsy Res* Suppl 8: 147–155, 1992.

59. Heinemann U, Lux HD, Gutnick MJ. Extracellular free calcium and potassium during paroxsmal activity in the cerebral cortex of the cat. *Exp Brain Res* 27: 237–243, 1977.

60. Hertz L, Chen Y, Spatz M. Involvement of non-neuronal brain cells in AVP-mediated regulation of water space at the cellular, organ, and whole-body level. *J Neurosci Res* 62: 480–490, 2000.

61. Hess D, El Manira A. Characterization of a high-voltage-activated IA current with a role in spike timing and locomotor pattern generation. *Proc Natl Acad Sci USA* 98: 5276–5281, 2001.

62. Hinterkeuser S, Schroder W, Hager G, Seifert G, Blumcke I, Elger CE, Schramm J, Steinhauser C. Astrocytes in the hippocampus of patients with temporal lobe epilepsy display changes in potassium conductances. *Eur J Neurosci* 12: 2087–2096, 2000.

63. Hochman DW, D'Ambrosio R, Janigro D, Schwartzkroin PA. Extracellular chloride and the maintenance of spontaneous epileptiform activity in rat hippocampal slices. *J Neurophysiol* 81: 49–59, 1999.

64. Hochman DW, Schwartzkroin PA. Chloride-cotransport blockade desynchronizes neuronal discharge in the "epileptic" hippocampal slice. *J Neurophysiol* 83: 406–417, 2000.

65. Hounsgaard J, Nicholson C. Potassium accumulation around individual purkinje cells in cerebellar slices from the guinea-pig. *J Physiol* 340: 359–388, 1983.

66. Huguenard JR. Low-threshold calcium currents in central nervous system neurons. *Ann Rev Physiol* 58: 329–348, 1996.

67. Huh Y, Cho J. Discrete pattern of burst stimulation in the ventrobasal thalamus for anti-nociception. *PLos One* 8: e67655, 2013.

68. Jasinski PE, Molkov YI, Shevtsova NA, Smith JC, Rybak IA. Sodium and calcium mechanisms of rhythmic bursting in excitatory neural networks of the pre-Botzinger complex: a computational modelling study. *Eur J Neurosci* 37: 212–230, 2013.

69. Jayakumar AR, Norenberg MD. The Na-K-Cl Cotransporter in astrocyte swelling. *Metab Brain Dis* 25: 31–38, 2010.

70. Jensen MS, Yaari Y. Role of intrinsic burst firing, potassium accumulation, and electrical coupling in the elevated potassium model of hippocampal epilepsy. *J Neurophysiol* 77: 1224–1233, 1997.

71. Ji H, Shepard PD. SK Ca^{2+}-activated K^+ channel ligands alter the firing pattern of dopamine-containing neurons in vivo. *Neuroscience* 140: 623–633, 2006.

72. Jinno S, Ishizuka S, Kosaka T. Ionic currents underlying rhythmic bursting of ventral mossy cells in the developing mouse dentate gyrus. *Eur J Neurosci* 17: 1338–1354, 2003.

73. Johnson SM, Smith JC, Funk GD, Feldman JL. Pacemaker behavior of respiratory neurons in medullary slices from neonatal rat. *J Neurophysiol* 72: 2598–2608, 1994.

74. Karus C, Mondragao MA, Ziemens D, Rose CR. Astrocytes restrict discharge duration and neuronal sodium loads during recurrent network activity. *Glia* 63: 936–957, 2015.

75. Kivi A, Lehmann TN, Kovacs R, Eilers A, Jauch R, Meencke HJ, von Deimling A, Heinemann U, Gabriel S. Effects of barium on stimulus-induced rises of $[K^+]_o$ in human epileptic non-sclerotic and sclerotic hippocampal area CA1. *Eur J Neurosci* 12: 2039–2048, 2000.

76. Kofuji P, Newman EA. Potassium buffering in the central nervous system. *Neuroscience* 129: 1045–1056, 2004.

77. Kroeger D, Tamburri A, Amzica F, Sik A. Activity-dependent layer-specific changes in the extracellular chloride concentration and chloride driving force in the rat hippocampus. *J Neurophysiol* 103: 1905–1914, 2010.

78. Kuhn AA, Trottenberg T, Kivi A, Kupsch A, Schneider GH, Brown P. The relationship between local field potential and neuronal discharge in the subthalamic nucleus of patients with Parkinson's disease. *Exp Neurol* 194: 212–220, 2005.

79. Kuhn AA, Williams D, Kupsch A, Limousin P, Hariz M, Schneider GH, Yarrow K, Brown P. Event-related beta desynchronization in human subthalamic nucleus correlates with motor performance. *Brain* 127: 735–746, 2004.

80. Langer J, Rose CR. Synaptically induced sodium signals in hippocampal astrocytes in situ. *J Physiol* 587: 5859–5877, 2009.

81. Lascola CD, Kraig RP. Whole-cell chloride currents in rat astrocytes accompany changes in cell morphology. *J Neurosci* 16: 2532–2545, 1996.

82. Latour I, Hamid J, Beedle AM, Zamponi GW, Macvicar BA. Expression of voltage-gated Ca^{2+} channel subtypes in cultured astrocytes. *Glia* 41: 347–353, 2003.

83. Launay P, Fleig A, Perraud AL, Scharenberg AM, Penner R, Kinet JP. TRPM4 is a Ca^{2+}-activated nonselective cation channel mediating cell membrane depolarization. *Cell* 109: 397–407, 2002.

84. Lee D. Coherent oscillations in neuronal activity of the supplementary motor area during a visuomotor task. *J Neurosci* 23: 6798–6809, 2003.

85. Lee DJ, Hsu MS, Seldin MM, Arellano JL, Binder DK. Decreased expression of the glial water channel aquaporin-4 in the intrahippocampal kainic acid model of epileptogenesis. *Exp Neurol* 235: 246–255, 2012.

86. Li Z, Hatton GI. Oscillatory bursting of phasically firing rat supraoptic neurones in low-Ca^{2+} medium: Na^+ influx, cytosolic Ca^{2+} and gap junctions. *J Physiol* 496: 379–394, 1996.

87. Lian XY, Stringer JL. Astrocytes contribute to regulation of extracellular calcium and potassium in the rat cerebral cortex during spreading depression. *Brain Res* 1012: 177–184, 2004.

88. Liao YF, Tsai ML, Chen CC, Yen CT. Involvement of the CaV3.2 T-type calcium channel in thalamic neuron discharge patterns. *Mol Pain* 7: 43, 2011.

89. Liu Y, Harding M, Pittman A, Dore J, Striessnig J, Rajadhyaksha A, Chen X. CaV1.2 CaV1.3 L-type calcium channels regulate dopaminergic firing activity in the mouse ventral tegmental area. *J Neurophysiol* 112: 1119–1130, 2014.

90. Luthi A, Bal T, McCormick DA. Periodicity of thalamic spindle waves is abolished by ZD7288,a blocker of Ih. *J Neurophysiol* 79: 3284–3289, 1998.

91. Luu P, Tucker DM, Makeig S. Frontal midline theta and the error-related negativity: neurophysiological mechanisms of action regulation. *Clin Neurophysiol* 115: 1821–1835, 2004.

92. MacGregor DJ, Leng G. Phasic firing in vasopressin cells: understanding its functional significance through computational models. *PLoS Comp Biol* 8: e1002740, 2012.

93. Maier JX, Neuhoff JG, Logothetis NK, Ghazanfar AA. Multisensory integration of looming signals by rhesus monkeys. *Neuron* 43: 177–181, 2004.

94. Mani RS, Boyes BE, Kay CM. Physicochemical and optical studies on calcium- and potassium-induced conformational changes in bovine brain S-100b protein. *Biochemistry* 21: 2607–2612, 1982.

95. Mani RS, Shelling JG, Sykes BD, Kay CM. Spectral studies on the calcium binding properties of bovine brain S-100b protein. *Biochemistry* 22: 1734–1740, 1983.

96. Marchetti C, Beato M, Nistri A. Evidence for increased extracellular K^+ as an important mechanism for dorsal root induced alternating rhythmic activity in the neonatal rat spinal cord in vitro. *Neurosci Lett* 304: 77–80, 2001.

97. Medici V, Frassoni C, Tassi L, Spreafico R, Garbelli R. Aquaporin 4 expression in control and epileptic human cerebral cortex. *Brain Res* 1367: 330–339, 2011.

98. Mirmiran M, Corner M. Neuronal discharge patterns in the occipital cortex of developing rats during active and quiet sleep. *Brain Res* 255: 37–48, 1982.

99. Moody WJ, Futamachi KJ, Prince DA. Extracellular potassium activity during epileptogenesis. *Exp Neurol* 42: 248–263, 1974.

100. Moraes DJ, da Silva MP, Bonagamba LG, Mecawi AS, Zoccal DB, Antunes-Rodrigues J, Varanda WA, Machado BH. Electrophysiological properties of rostral ventrolateral medulla presympathetic neurons modulated by the respiratory network in rats. *J Neurosci* 33: 19223–19237, 2013.

101. Morquette P, Verdier D, Kadala A, Fethiere J, Philippe AG, Robitaille R, Kolta A. An astrocyte-dependent mechanism for neuronal rhythmogenesis. *Nat Neurosci* 18: 844–854, 2015.

102. Mrejeru A, Wei A, Ramirez JM. Calcium-activated non-selective cation currents are involved in generation of tonic and bursting activity in dopamine neurons of the substantia nigra pars compacta. *J Physiol* 589: 2497–2514, 2011.

103. Muller M, Schlue WR. Macroscopic and single-channel chloride currents in neuropile glial cells of the leech central nervous system. *Brain Res* 781: 307–319, 1998.

104. Muramatsu Y, Kurosaki R, Watanabe H, Michimata M, Matsubara M, Imai Y, Araki T. Expression of S-100 protein is related to neuronal damage in MPTP-treated mice. *Glia* 42: 307–313, 2003.

105. Nagelhus EA, Mathiisen TM, Ottersen OP. Aquaporin-4 in the central nervous system: cellular and subcellular distribution and coexpression with KIR4.1. *Neuroscience* 129: 905–913, 2004.

106. Neckelmann D, Amzica F, Steriade M. Spike-wave complexes and fast components of cortically generated seizures. III. Synchronizing mechanisms. *J Neurophysiol* 80: 1480–1494, 1998.

107. Neprasova H, Anderova M, Petrik D, Vargova L, Kubinova S, Chvatal A, Sykova E. High extracellular K^+ evokes changes in voltage-dependent K^+ and Na^+ currents and volume regulation in astrocytes. *Pflügers Arch* 453: 839–849, 2007.

108. Newman EA, Zahs KR. Modulation of neuronal activity by glial cells in the retina. *J Neurosci* 18: 4022–4028, 1998.

109. Nicholson C, Bruggencate GT, Steinberg R, Stockle H. Calcium modulation in brain extracellular microenvironment demonstrated with ion-selective micropipette. *Proc Natl Acad Sci USA* 74: 1287–1290, 1977.

110. Nishimura Y, Asahi M, Saitoh K, Kitagawa H, Kumazawa Y, Itoh K, Lin M, Akamine T, Shibuya H, Asahara T, Yamamoto T. Ionic mechanisms underlying burst firing of layer III sensorimotor cortical neurons of the cat: an in vitro slice study. *J Neurophysiol* 86: 771–781, 2001.

111. Noda H, Mikami A. Discharges of neurons in the dorsal parafloccullus of monkeys during eye movements and visual stimulation. *J Neurophysiol* 56: 1129–1146, 1986.

112. O'Connor ER, Sontheimer H, Spencer DD, de Lanerolle NC. Astrocytes from human hippocampal epileptogenic foci exhibit action potential-like responses. *Epilepsia* 39: 347–354, 1998.

113. Oke OO, Magony A, Anver H, Ward PD, Jiruska P, Jefferys JG, Vreugdenhil M. High-frequency gamma oscillations coexist with low-frequency gamma oscillations in the rat visual cortex in vitro. *Eur J Neurosci* 31: 1435–1445, 2010.

114. Onimaru H, Arata A, Homma I. Intrinsic burst generation of preinspiratory neurons in the medulla of brainstem-spinal cord preparations isolated from newborn rats. *Exp Brain Res* 106: 57–68, 1995.

115. Orkand RK, Nicholls JG, Kuffler SW. Effect of nerve impulses on the membrane potential of glial cells in the central nervous system of amphibia. *J Neurophysiol* 29: 788–806, 1966.

116. Pace RW, Mackay DD, Feldman JL, Del Negro CA. Inspiratory bursts in the preBotzinger complex depend on a calcium-activated non-specific cation current linked to glutamate receptors in neonatal mice. *J Physiol* 582: 113–125, 2007.

117. Panaitescu B, Ruangkittisakul A, Ballanyi K. Silencing by raised extracellular Ca^{2+} of pre-Botzinger complex neurons in newborn rat brainstem slices without change of membrane potential or input resistance. *Neurosci Lett* 456: 25–29, 2009.

118. Payne JA, Rivera C, Voipio J, Kaila K. Cation-chloride co-transporters in neuronal communication, development and trauma. *Trends Neurosci* 26: 199–206, 2003.

119. Pena F, Parkis MA, Tryba AK, Ramirez JM. Differential contribution of pacemaker properties to the generation of respiratory rhythms during normoxia and hypoxia. *Neuron* 43: 105–117, 2004.

120. Perez-Reyes E. Molecular physiology of low-voltage-activated t-type calcium channels. *Physiol Rev* 83: 117–161, 2003.

121. Pinto DJ, Patrick SL, Huang WC, Connors BW. Initiation, propagation, and termination of epileptiform activity in rodent neocortex in vitro involve distinct mechanisms. *J Neurosci* 25: 8131–8140, 2005.

122. Putzier I, Kullmann PH, Horn JP, Levitan ES. CaV1.3 channel voltage dependence, not Ca^{2+} selectivity, drives pacemaker activity and amplifies bursts in nigral dopamine neurons. *J Neurosci* 29: 15414–15419, 2009.

123. Ransdell JL, Temporal S, West NL, Leyrer ML, Schulz DJ. Characterization of inward currents and channels underlying burst activity in motoneurons of crab cardiac ganglion. *J Neurophysiol* 110: 42–54, 2013.

124. Reyes RC, Verkhratsky A, Parpura V. Plasmalemmal Na^+/Ca^{2+} exchanger modulates Ca^{2+}-dependent exocytotic release of glutamate from rat cortical astrocytes. *ASN Neuro* 4: 2012.

125. Richter DW, Camerer H, Sonnhof U. Changes in extracellular potassium during the spontaneous activity of medullary respiratory neurones. *Pflügers Arch* 376: 139–149, 1978.

126. Robinson RB, Siegelbaum SA. Hyperpolarization-activated cation currents: from molecules to physiological function. *Ann Rev Physiol* 65: 453–480, 2003.

127. Rojas H, Ramos M, Benaim G, Caputo C, DiPolo R. The activity of the Na^+/Ca^{2+} exchanger largely modulates the $Ca^{2+}{}_i$ signal induced by hypo-osmotic stress in rat cerebellar astrocytes. The effect of osmolarity on exchange activity. *J Physiol Sci* 58: 277–279, 2008.

128. Rose CR, Karus C. Two sides of the same coin: sodium homeostasis and signaling in astrocytes under physiological and pathophysiological conditions. *Glia* 61: 1191–1205, 2013.

129. Rose CR, Ransom BR. Regulation of intracellular sodium in cultured rat hippocampal neurones. *J Physiol* 499: 573–587, 1997.

130. Rubin JE, Hayes JA, Mendenhall JL, Del Negro CA. Calcium-activated nonspecific cation current and synaptic depression promote network-dependent burst oscillations. *Proc Natl Acad Sci USA* 106: 2939–2944, 2009.

131. Rubino D, Robbins KA, Hatsopoulos NG. Propagating waves mediate information transfer in the motor cortex. *Nat Neurosci* 9: 1549–1557, 2006.

132. Rybak IA, Shevtsova NA, St-John WM, Paton JF, Pierrefiche O. Endogenous rhythm generation in the pre-Botzinger complex and ionic currents: modelling and in vitro studies. *Eur J Neurosci* 18: 239–257, 2003.

133. Sakatani S, Seto-Ohshima A, Itohara S, Hirase H. Impact of S100B on local field potential patterns in anesthetized and kainic acid-induced seizure conditions in vivo. *Eur J Neurosci* 25: 1144–1154, 2007.

134. Sakatani S, Seto-Ohshima A, Shinohara Y, Yamamoto Y, Yamamoto H, Itohara S, Hirase H. Neural-activity-dependent release of S100B from astrocytes enhances kainate-induced gamma oscillations in vivo. *J Neurosci* 28: 10928–10936, 2008.

135. Sathe K, Maetzler W, Lang JD, Mounsey RB, Fleckenstein C, Martin HL, Schulte C, Mustafa S, Synofzik M, Vukovic Z, Itohara S, Berg D, Teismann P. S100B is increased in Parkinson's disease and ablation protects against MPTP-induced toxicity through the RAGE and TNF-alpha pathway. *Brain* 135: 3336–3347, 2012.

136. Scemes E, Spray DC. Extracellular K^+ and astrocyte signaling via connexin and pannexin channels. *Neurochem Res* 37: 2310–2316, 2012.

137. Schnell C, Fresemann J, Hulsmann S. Determinants of functional coupling between astrocytes and respiratory neurons in the pre-Botzinger complex. *PLos One* 6: e26309, 2011.

138. Sederberg PB, Schulze-Bonhage A, Madsen JR, Bromfield EB, McCarthy DC, Brandt A, Tully MS, Kahana MJ. Hippocampal and neocortical gamma oscillations predict memory formation in humans. *Cereb Cortex* 17: 1190–1196, 2007.

139. Sharott A, Doig NM, Mallet N, Magill PJ. Relationships between the firing of identified striatal interneurons and spontaneous and driven cortical activities in vivo. *J Neurosci* 32: 13221–13236, 2012.

140. Somjen GG. Extracellular potassium in the mammalian central nervous system. *Ann Rev Physiol* 41: 159–177, 1979.

141. Somjen GG, Muller M. Potassium-induced enhancement of persistent inward current in hippocampal neurons in isolation and in tissue slices. *Brain Res* 885: 102–110, 2000.

142. Sontheimer H. Voltage-dependent ion channels in glial cells. *Glia* 11: 156–172, 1994.

143. Spain WJ, Schwindt PC, Crill WE. Anomalous rectification in neurons from cat sensorimotor cortex in vitro. *J Neurophysiol* 57: 1555–1576, 1987.

144. Steriade M, Nunez A, Amzica F. Intracellular analysis of relations between the slow (<1 Hz) neocortical oscillation and other sleep rhythms of the electroencephalogram. *J Neurosci* 13: 3266–3283, 1993.

145. Stockle H, Ten Bruggencate G. Fluctuation of extracellular potassium and calcium in the cerebellar cortex related to climbing fiber activity. *Neuroscience* 5: 893–901, 1980.

146. Su H, Alroy G, Kirson ED, Yaari Y. Extracellular calcium modulates persistent sodium current-dependent burst-firing in hippocampal pyramidal neurons. *J Neurosci* 21: 4173–4182, 2001.

147. Subbarao KV, Stolzenburg JU, Hertz L. Pharmacological characteristics of potassium-induced, glycogenolysis in astrocytes. *Neurosci Lett* 196: 45–48, 1995.

148. Tas PW, Massa PT, Kress HG, Koschel K. Characterization of an $Na^+/K^+/Cl^-$ co-transport in primary cultures of rat astrocytes. *Biochim Biophys Acta* 903: 411–416, 1987.

149. Tazerart S, Vinay L, Brocard F. The persistent sodium current generates pacemaker activities in the central pattern generator for locomotion and regulates the locomotor rhythm. *J Neurosci* 28: 8577–8589, 2008.

150. Thimm J, Mechler A, Lin H, Rhee S, Lal R. Calcium-dependent open/closed conformations and interfacial energy maps of reconstituted hemichannels. *J Biol Chem* 280: 10646–10654, 2005.

151. Trevelyan AJ, Sussillo D, Watson BO, Yuste R. Modular propagation of epileptiform activity: evidence for an inhibitory veto in neocortex. *J Neurosci* 26: 12447–12455, 2006.

152. Tsuruyama K, Hsiao CF, Chandler SH. Participation of a persistent sodium current and calcium-activated nonspecific cationic current to burst generation in trigeminal principal sensory neurons. *J Neurophysiol* 110: 1903–1914, 2013.

153. Uhlhaas PJ, Singer W. Neural synchrony in brain disorders: relevance for cognitive dysfunctions and pathophysiology. *Neuron* 52: 155–168, 2006.

154. Ullrich ND, Voets T, Prenen J, Vennekens R, Talavera K, Droogmans G, Nilius B. Comparison of functional properties of the Ca^{2+}-activated cation channels TRPM4 and TRPM5 from mice. *Cell Calcium* 37: 267–278, 2005.

155. Van Eldik LJ, Zimmer DB. Secretion of S-100 from rat C6 glioma cells. *Brain Res* 436: 367–370, 1987.

156. Vega-Saenz de Miera EC, Rudy B, Sugimori M, Llinas R. Molecular characterization of the sodium channel subunits expressed in mammalian cerebellar Purkinje cells. *Proc Natl Acad Sci USA* 94: 7059–7064, 1997.

157. Verkhratsky A, Steinhauser C. Ion channels in glial cells. *Brain Res Brain Res Rev* 32: 380–412, 2000.

158. Wallen P, Grafe P, Grillner S. Phasic variations of extracellular potassium during fictive swimming in the lamprey spinal cord in vitro. *Acta Physiol Scand* 120: 457–463, 1984.

159. Wang XJ. Neurophysiological and computational principles of cortical rhythms in cognition. *Physiol Rev* 90: 1195–1268, 2010.

160. Westenbroek RE, Bausch SB, Lin RC, Franck JE, Noebels JL, Catterall WA. Upregulation of L-type Ca^{2+} channels in reactive astrocytes after brain injury, hypomyelination, and ischemia. *J Neurosci* 18: 2321–2334, 1998.

161. Xu L, Zeng LH, Wong M. Impaired astrocytic gap junction coupling and potassium buffering in a mouse model of tuberous sclerosis complex. *Neurobiol Disease* 34: 291–299, 2009.

162. Xu W, Lipscombe D. Neuronal Ca(V)1.3alpha(1) L-type channels activate at relatively hyperpolarized membrane potentials and are incompletely inhibited by dihydropyridines. *J Neurosci* 21: 5944–5951, 2001.

163. Zanotti S, Charles A. Extracellular calcium sensing by glial cells: low extracellular calcium induces intracellular calcium release and intercellular signaling. *J Neurochem* 69: 594–602, 1997.

164. Zhang B, Wootton JF, Harris-Warrick RM. Calcium-dependent plateau potentials in a crab stomatogastric ganglion motor neuron. II. Calcium-activated slow inward current. *J Neurophysiol* 74: 1938–1946, 1995.